Resonant tunneling transport in AlxGa1-x/InyGa1-yN/ AlxGa1-x/ InzGa1-zN quantum structures

A Bhouri, A Rached, J.-L. Lazzari

Resonant tunneling transport in $Al_xGa_{1-x}/In_yGa_{1-y}N/ Al_xGa_{1-x}/ In_zGa_{1-z}N$ quantum structures

A. Bhouri[1], A. Rached[1], and J. L. lazzari[2]

[1] Laboratoire d'Electronique et Microélectronique, Faculté des Sciences de Monastir, 5019 Monastir, Tunisia.

[2] Centre Interdisciplinaire de Nanoscience de Marseille (CINaM), UPR-CNRS 3118, Aix-Marseille Université, Case 913, Campus de Luminy, 13288 Marseille cedex 9, France

Abstract

In this work, we present room temperature simulation of the vertical electron transport in the pseudomorphic quantum stack $Al_{0.5}G_{0.5}N/In_xGa_{1-x}N/Al_{0.5}G_{0.5}N/In_{0.1}Ga_{0.9}N/GaN$ that is designed with a 6nm thick lateral $In_{0.1}Ga_{0.9}N/GaN$ n-type corrected spacer. Using the transfer matrix formalism, we investigate the effect of the conduction band discontinuities and internal field on the transmission coefficient and the current-voltage characteristics by varying indium contents in the central quantum well. We demonstrate that an optimal design in terms of compositions, thicknesses and doping of the studied resonant tunneling structure may allow a peak-to-valley ratio (PVR) as high as 882 @1.1-1.3Volts.

Key words: Nitride materials, Piezoelectricity, Quantum Wells, Resonant Tunneling Diodes, Peak to Valley Ratio.

Corresponding author: Bhouri_amel@yahoo.fr

Tel :+216 52 67 60 42

1 INTRODUCTION

During the past decades, a tremendous theoretical and experimental research effort has been invested in the field of nanostructured optoelectronic devices based on III-nitride materials and their alloys. Electronic and optical properties of GaN and related materials make them suitable for a variety of application such as laser and light emitting diodes in blue-green and ultra- violet spectral range [1]. Due to large values of the conduction band discontinuity (1.75 eV between GaN and AlN) and very short intersubband (ISB) relaxation times measured in femtoseconds, GaN/Al(Ga)N nanostructures have become the system of choice for near-infrared ISB devices [2]. Moreover, thanks to the high energy of their longitudinal optical phonon modes (92 meV in GaN), III-nitrides are excellent candidates for the fabrication of high temperature THz quantum cascade lasers (QCLs) [3]. All these key applications require the study of vertical transport using basically the double-barrier (DB) Resonant Tunneling Diode (RTD).

For wurtzite AlGaN/GaN structures grown in the c-plane direction, the band profile is distinguished by huge internal electric fields. These built-in fields arise from the interface charges originating in spontaneous and piezoelectric polarization [4,5]. The internal electric fields associated with polarizations lead to the formation of a two dimensional electron gas (2DEG) specified by a shallow triangular sharped well within the left side contact of the RTD and a depleted region on the right side [6]. The peculiarly induced polarization effects, formed at the two sides of the active region, exacerbate the challenge for numerous applications in electron devices based on vertical electron transport.

AlGaN/GaN RTD have increasingly become important due to its high frequency performance and capability of providing negative differential resistance at room temperature (NDR). The large NDR observed at Room Temperature in AlGaN/GaN diode has been interpreted as related to the sequential resonant tunneling process and is found to be sensitive to the internal electric field present in III-nitride compounds and to the depleted space charge GaN region [7]. In fact, the band bending in the depletion region sets up a barrier which may seriously impede perpendicular electronic transport. This may ruin the performance of devices such as quantum-cascade lasers and resonant-tunneling diodes.

For device applications, it is important to understand how the different properties of the RTD (e.g. peak currents, valley current and peak voltage Ratio (PVR)) are controlled by the crystal layout such as well width, barrier size and doping concentration. Thus, the

optimization of these parameters is of great interest with the aim to improve the performance of devices.

In this study we propose studying the electronic properties of $(In_x)Ga_{1-x}N/Al_{0.5}Ga_{0.5}N$ double barrier RTD. We also intend to improve the main properties of the RTD through polarization modulation using a heavily doped $In_{0.1}Ga_{0.9}N$ layer which introduces an additional polarization field beyond the Second barrier. We show that our self consistent calculations first illustrate that this design can effectively minimize the depleted space charge region in the right-hand contact layer and furthermore, we demonstrate that an appropriate choice of thicknesses, doping and compositions of these resonant tunneling diodes may allow a peak current density as high as 7.73×10^5 A/cm^2 and a pronounced 882 PVR value arising from the enhancement of the peak current.

The paper is organized as follow: In Section 2, we give a brief description of the theoretical model used in our calculations. Then we report in section 3 our results obtained on RTD conduction band profiles, transmission probabilities and J-V characteristics followed by a discussion of the influence of Indium composition, barrier and well width and also of the doping concentration on the RTD proprieties. Conclusions are summarized in Section 4.

2-THEORITICAL APPROACH

The conduction band profiles, free-electron distribution and the electron eigenstates are calculated self consistently by solving the one–electron Schrodinger equation within the effective mass and Hartree approximations**,** along with the Poisson equation for the structure under consideration. Along the growth direction (z axis), the Schrödinger equation is expressed as:

$$\left[-\frac{\hbar^2}{2}\frac{\partial}{\partial \mathrm{z}}\left(\frac{1}{\mathrm{m(z)}}\frac{\partial}{\partial \mathrm{z}}\right)+\mathrm{V(z)}\right]\psi_n(\mathrm{z})=\mathrm{E}_n\psi_n(\mathrm{z}) \quad (1)$$

where E_n and $\psi_n(\mathrm{z})$ are the energy level and wave function of the nth subband respectively, $\mathrm{m(z)}$ is the position-dependent electron effective mass and $V(z)$ is the electron potential energy such as:

$$V(\mathrm{z})=V_0(z)+V_{sc}(z) \quad (2)$$

$V_0(z)$ is the potential energy before the charge transfer. The Poisson equation is given by:

$$-\frac{\partial}{\partial}\left(\varepsilon\frac{\partial V_{sc}}{\partial z}\right)=\rho(z) \quad (3)$$

We note that the term $V_{sc}(z)$ incorporates the potential function including the effect of the spontaneous and piezoelectric polarizations and $\rho(z)$ is the charge distributions given by:

$$\rho(z) = \mathrm{q}(\mathrm{N_D(z)} - \mathrm{n(z)}) \quad (4)$$

where, $\varepsilon(\mathrm{z})$ is the position-dependent dielectric constant, $\mathrm{N_D}$ (z) is the ionized donor doping concentration and $\mathrm{n(z)}$ is the free-electron concentration.

Based on the general formalism for calculating band structure of semiconductor heterostructures, finite difference method is applied to solve Schrödinger and Poisson equations. The one dimension (1D) real space along the studied structure has been divided into discrete non uniform mesh points and the latter equations have been written within these discrete spacing principally in the active area and semi-infinite contacts. For self consistent calculations, a closed loop is formed to solve the Schrödinger and Poisson equation alternately until convergence.

The transfer matrix approach, which is suitable for treating arbitrary potential barriers, is used to model the tunneling current density $J - V$ [8]. In our calculations, we assume ballistic transport. Based on Tsu–Esaki formalism [9], the local current density can be described following the expression:

$$\mathrm{J(V_a)} = \left(\mathrm{emk_\beta T}/2\pi^2\hbar^3\right) \times \int_0^\infty \mathrm{T(E)Ln}\left(\frac{1+\exp(\mathrm{E_F}-\mathrm{E}/\mathrm{k_\beta T})}{1+\exp(\mathrm{E_F}-\mathrm{E}-\mathrm{eV_a}/\mathrm{k_\beta T})}\right) \quad (5)$$

here, V_a is the applied voltage across the active region, , E_F is the energy Femi level and $T(E)$ is the transmission coefficient calculated for the specific value of $\mathrm{V_a}$.

2-RESULTS AND DISCUSSION

We start this work by studying conduction band diagram and electronic characteristics of a conventional and symmetric double barrier single well AlGaN/GaN RTD in the wurtzite structure. The symmetric RTD structure consist of an active region sandwiched between n^+ (5.10^{18} cm^{-3}) bottom and top GaN contacts with 95 nm width. The active region is composed by a single 2 nm thick undoped GaN QW enclosed by two 1 nm thick undoped $Al_{0.5}Ga_{0.5}N$ barriers. The active region is followed by 5 nm thick undopped GaN spacers. The GaN spacers are included to prevent the presence of carriers in the quantum well since a nonzero well occupancy with no applied bias would violate the validity of the coherent transport inhibit the performance of the RTD. For wurtzite AlGaN/(In)GaN heterostructures,

both constituent materials have only one conduction band minimum at the center of the Brillouin zone. The effective masses and the other related parameters are given in table 1.

Table 1: GaN, AlN and InN physical parameters

Parameters	GaN	AlN	InN
a (Å)	3,189[10]	3,112[10]	3,545[10]
c (Å)	5,185[10]	4,982[10]	5,703[10]
E_g (eV)	3,39[12]	6,2[13]	0,78[10]
$m_e^{\|\|}$	0,2[10]	0,32[10]	0,07[10]
$\varepsilon_{stat}^{\|\|}$	10,1[14]	8,5[15]	14,61[16]
C_{13}(GPa)	106 [16]	108[16]	92[16]
C_{33} (GPa)	398[11]	373[11]	224[16]
e_{31} (C/m^2)	-0,35[11]	-0,5[11]	-0,41[16]
e_{33} (C/m^2)	1,27[11]	1,79[11]	0,81[16]
P_{sp}(C/m^2)	-0,029[11]	-0,081[11]	-0,032[11]

The curve displayed in figure 1(a) (black line) represents the simulated equilibrium conduction band diagram of such symmetric RTD. The zero energy level was arbitrarily placed at the bottom of the conduction band on the left contact and the energy Fermi level has been calculated to be close to $0.04\ eV$. As it can be seen, the spontaneous and piezoelectric polarizations induce a strong asymmetry in the conduction band profile despite symmetrical barrier geometry. The effect of the two polarization components on the morphology of the structure is very noticeable mainly the formation of a triangular confinement potentials. Indeed, the electric fields are non-zero in the well and in the barriers and have opposite signs leading to an effectively triangular confinement potential [4]. Moreover, the polarization difference between the materials GaN and AlGaN induces a positive charge at the AlGaN/GaN interface. Free electrons are attracted by this positive charge and tend to accumulate in a quantum well close to the interface.

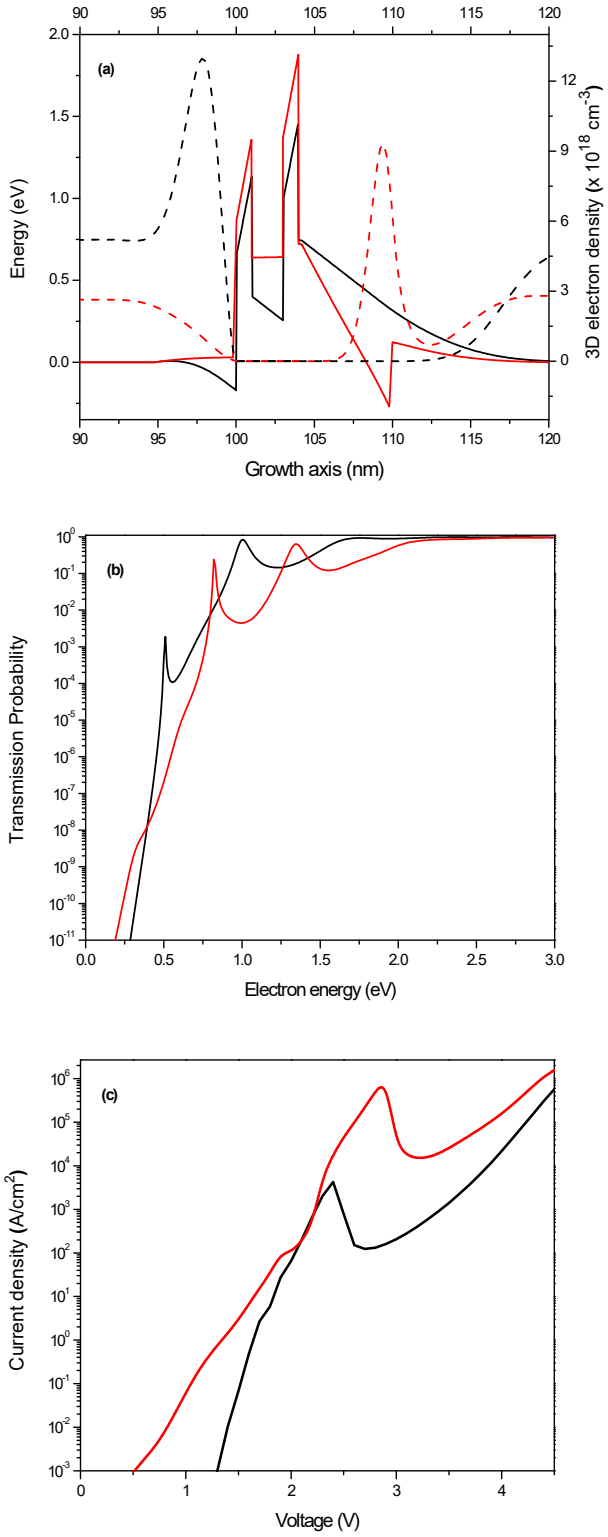

Figure 1: Results of Self consistent calculation of: (a) equilibrium conduction band edges and free electro density at zero bias, (b) transmission probabilities and (c) current densities of n^+ GaN/GaN/$Al_{0.5}G_{0.5}N$/GaN/$Al_{0.5}G_{0.5}N$/GaN/n^+ GaN quantum structure (solid black lines) and of n^+ GaN/GaN/$Al_{0.5}G_{0.5}N$/GaN/$Al_{0.5}G_{0.5}N$/n^+ GaN 6nm $In_{0.1}Ga_{0.9}N$/n^+ GaN structure (solid red lines). The doping concentration is equal to 5.10^{18} cm^{-3}.

For the unbiased double barrier structure, the internal electric field associated with these polarizations lead to the formation of a two dimensional electron gas (2DEG) specified by a sharped well (inversion region) within the left reservoir region, and a depletion region on the right side of the active region. We note that the formation of depletion and inversion regions in the conduction band is the sole mechanism responsible for securing equilibrium.

The transmission coefficient $T(E)$ for the $Al_{0.5}Ga_{0.5}N$/GaN symmetric RTD is then obtained with the transfer-matrix method and represented in fig.1 (b) (black line). The transmission coefficient shows two resonant peaks. The first peak, located at $0.51\ eV$, is attributed to the resonant tunneling through the fundamental quasi-bound state in the QW. The second peak is due to the tunneling through the excited quasi-bound state or a continuum state near the DB edge and is positioned at $1.0\ eV$.

The current density-voltage is simulated on the basis of eq. 5. Bias voltage refers to the one applied on the top contact. The $J-V$ characteristic is plotted on fig. 1(c) (black line). At room temperature, we calculate a PVR value of about 29. Despite the large conduction band offset between $Al_{0.5}Ga_{0.5}N$ and GaN ($\approx 0.73\ eV$), the obtained PVR value is considered relatively small. The main factor that limits the performance of the GaN based RTD is noted from the calculated conduction band profile at equilibrium (figure 1(a)). In fact, the depletion region in the conduction band, which is typically of a wide spatial dimension, has a significant current-impeding effect. The presence of such depletion region assumes that the electron density is considerably low on the right side of the second barrier. In order to confirm this supposition, room temperature local density of confined electrons is performed in the whole structure as it is shown in figure 1(a) (dashed black lines). At zero bias, we can observe that the local electron density appears negligible in the QW and also beyond it to the right-hand side. By contrast, we can note a high electron sheet density localized in the 2DEG channel at the GaN/$Al_{0.5}Ga_{0.5}N$ left interface. Therefore, the enhancement of the PVR is mainly related to the valley and peak current and to the asymmetry conduction band profile induced by polarization effects. This problem can be avoided if we use an InGaN layer following the $Al_{0.5}Ga_{0.5}N$ top barrier. Such a layer would increase the electron density on the wright contact region, minimize the depletion region, reduces the series resistance of the device and then increases the peak current.

In this context, we propose to substitute the 5 nm undoped spacer in the right side of the symmetric RTD structure by a heavily doped 6 nm $In_{0.1}Ga_{0.9}N$ lateral quantum well. The calculated conduction band profile (solid red line) and the local electron density (dashed red

line) of such new structure are displayed in figure 1(a). In comparison with the symmetric RTD, one can observe that the 2DEG inversion region within the left reservoir vanishes and the band becomes almost flat. Moreover, the width of the depletion region is reduced and the central QW resonant levels are pushed far from the conduction band edge in the contact layers. Thus, the device structure tends to become more symmetric. As expected, the calculated electron sheet density in the left-hand side contact region is strongly reduced, the GaN central QW remains unpopulated and a considerably high local electron density appears in the right contact region.

The calculated transmission coefficient of such proposed structure is presented in fig. 1(b) (solid black line). They support the later results obtained on conduction band diagram. In fact, the first and second resonant peaks are shifted to higher energy in comparison with those calculated, in the symmetric RTD, and are located at $0.82\ eV$ and $1.35\ eV$ respectively. The simulated $J-V$ curve displayed in fig.1(c) (solid red line) shows that both peak and valley currents are significantly increased in comparison with the conventional previously studied RTD. The effect of the corrected $In_{0.1}Ga_{0.9}N$ appears strong so that the peak and valley currents are about ten and four times, respectively, larger than those calculated in the symmetric $Al_{0.5}Ga_{0.5}$/GaN RTD. These effects enhance sharply the PVR which reaches a value of about 62. The obtained results open the possibility of proposing other structures that can minimize the depletion region, avoiding the 2DEG, which may prohibit the design of realistic structures, and maximizing the peak current and the PVR value.

As we have mentioned above, the smaller band gap of the InGaN corrected spacer is responsible on the accumulation and the increase of electron density at the collector region. We suggest now, using $In_xGa_{1-x}N$ alloy as the central QW material instead of the binary GaN in the aim to optimize and improve the performance of RTD structure. The active region of the corrected RTD heterostructure proposed now consists of $(L_Q\ nm)$-$In_xGa_{1-x}N$ quantum well enclosed by two $(L_B\ nm)$-$Al_{0.5}Ga_{0.5}$ barriers. The barriers are followed by 5 nm undoped first GaN spacer layer (left side) and 6nm-thick lateral n-type $In_{0.1}Ga_{0.9}N$ corrected spacer embedded at the right side region between the barrier and the upper GaN contact layer as can be seen in figure 2 (corrected RTD). The n-doped GaN contact layers are $95\ nm$-thick. The indium composition x, the layer thicknesses ($L_{Q,}\ L_B$) and the doping concentration (N_D) will be treated as parameters. These parameters should be optimized with the aim to improve and maximize the PVR which is considered as an essential parameter describing the quality of resonant tunneling diodes.

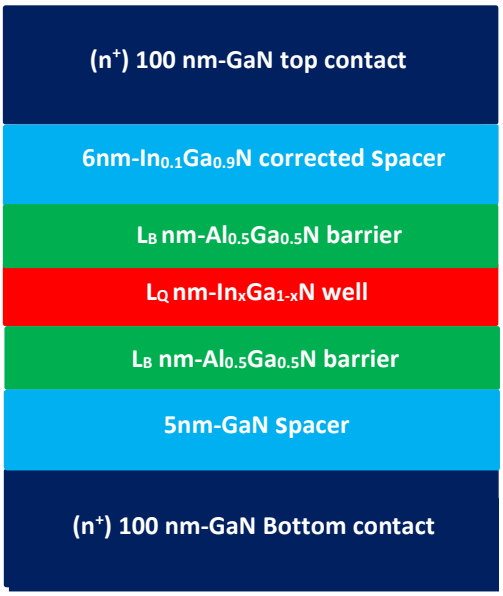

Figure 2: Schematic layer structure of the corrected resonant tunneling diodes.

3-1 Indium composition effects

We will consider a first structure series (A) consisting on the corrected RTD structure with indium composition x varying from 0 to 0.15, and with constant thickness layers ($L_B = 1\ nm, L_Q = 2\ nm$). The doping concentration N_D is equal to $5 \times 10^{18}\ cm^{-3}$. We note that in this case, the conduction band offset between $Al_{0.5}Ga_{0.5}N$ and GaN materials, the height of the barriers and the polarization induced electric fields are controlled by the amount of indium in the well. At room temperature, the self consistent calculations of unbiased potential profiles for the selected indium composition are displayed in figure 3(a). For a second time, the results show that the internal electric field breaks the symmetry of the unbiased potential profile. Moreover, as it can be noted, using $In_xGa_{1-x}N$ alloyed central QW, a new depletion region develops at the left hand reservoir and becomes more larger as the indium composition x augments. However, the right depletion region shortens when the indium composition increases. We point out that the formed depletion regions in the contact layers are unlike. Therefore, we expect that, there is a significant band filling of the active region which generates these two depletion regions. In fact, the $In_xGa_{1-x}N$ alloyed central QW together with the $In_{0.1}Ga_{0.9}N$ lateral corrected spacer ensure efficient filling of the active region rather than of the 2DEG at the $GaN/Al_{0.5}Ga_{0.5}N$ interface.

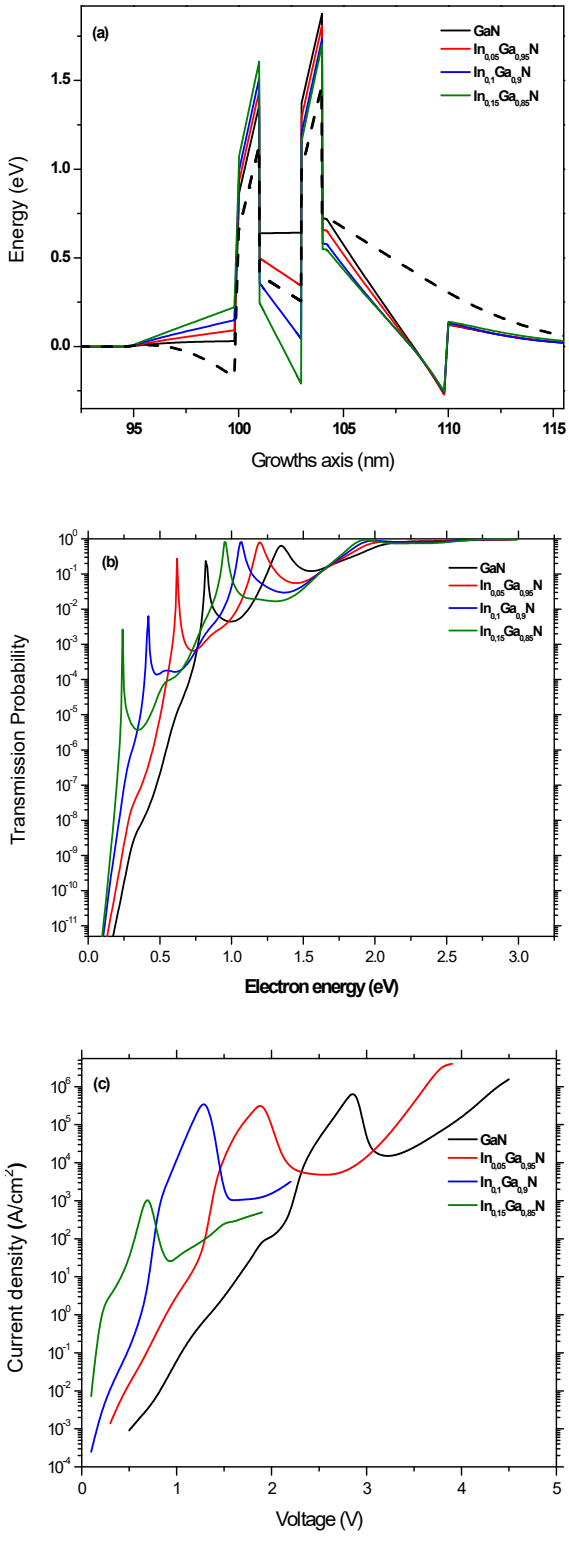

Figure 3: Results of: (a) Self consistent calculation of the equilibrium conduction band edge at zero bias, (b) transmission probability, and (c) current density for different In compositions in the n^+ (5.10^{18} cm^{-3})–GaN/5nm GaN/1 nm $Al_{0.5}G_{0.5}N$ /2 nm $In_xGa_{1-x}N$ /1 nm $Al_{0.5}G_{0.5}N$ / n^+ (5.10^{18} cm^{-3}) 6nm $In_{0.1}Ga_{0.9}N$ / n^+ (5.10^{18} cm^{-3}) GaN quantum structures.

The results of our computational transmission coefficient are displayed in fig. 3(b). All the transmission curves present two peaks resulting from the resonant tunneling through the quasibound states in the central InGaN QW. It is shown that when increasing x, the resonant peaks are shifted towards lower energy and their corresponding transmission values significantly decrease. To interpret the redshift in the resonance peaks, we compare the transmission curves with the conduction band profiles. It is clear that the position of the QWs and the double barriers are reliant on the internal electric field, itself dependent on indium composition because of the variation of the polarization discontinuity between $Al_{0.5}Ga_{0.5}N$ barrier and $In_xGa_{1-x}N$ QW. As it can be seen from fig. 3(a), the central QW is pushed down nearby the conduction band edge in the contact layers, leading to a redshift of the resonant peaks.

For calculating the current density, we apply a positive bias on the right-hand contact. The results displayed in fig. 2(c) show that as x increases, the current peaks progressively shift to lower voltages. The peak and valley currents are affected by indium compositions particularly when molar fraction x exceeds 10%. All the particular values extracted from $J-V$ characteristics are given in table 2. As one can notice, the valley current value is strongly reduced as x increases, however the peak current values don't follow a uniform change.

In summarize, we demonstrate that an appropriate choice of a 10% In composition achieves a peak current density of 5.72×10^5 A/cm^2 and a pronounced 564 PVR value which arises from the large decrease in the valley current.

Table 2: Values of $J-V$ calculation of the heterostructures of series (A) at 300 K.

Series(A) (L_B, L_Q) = (1nm, 2nm)	**x (%)**	**Current density** (A/cm^2)		**Tension** (V)		**PVR**
		Peak	Valley	Peak	Valley	
A1	0	$9{,}04\times10^5$	$1{,}46\times10^4$	2,9	3,2	62
A2	5	$4{,}3\times10^5$	$4{,}8\times10^3$	1,9	2,6	90
A3	**10**	$\mathbf{5{,}72\times10^5}$	$\mathbf{1{,}01\times10^3}$	**1,3**	**1,6**	**564**
A4	15	$2{,}57\times10^3$	19,56	0,7	0,9	131,4

3-2 Layer thicknesses effects

The following point is addressed to the study of the influence of layer thicknesses on the electronic transport in resonant tunneling diodes. We study the same structure defined in section 3-1 (figure 2) and we consider these new layer thicknesses ($L_B = 0.6\,nm, L_Q = 0.8\,nm$). We will note these structures as the second series (B) of corrected RTD. The doping concentration is also taken equal to $5 \times 10^{18}\,cm^{-3}$. The corresponding conduction band profiles are depicted in figure 4(a) where it can be seen that the internal fields breaks the symmetry and tow depletion regions are formed between the bottom (top) contact and the left (right) barrier respectively. The energy positions of the barriers and contacts are weakly affected by indium composition. However the quantum well is strongly influenced and is pushed down near the band position in the contact layers as x increases.

One can remark that the transmission curves, displayed in figure 4(b), present only one resonant peak, indicating that the tunneling occurs uniquely through the fundamental quasibound state in the quantum well. These results show that, taking the barrier and the well thicknesses equal to $0.6\,nm$ and $0.8\,nm$ respectively, the structures present only one resonant state for all the selected indium composition. Moreover the transmission peak intensity is slightly affected by composition and the peaks are not sharp meaning that the resonant state in the well is considerably above the Fermi level in the bottom contact layer.

Figure 4(c) shows that the current peak progressively shifts to lower voltages with increasing In content. The PVR is also strongly affected by x and increases with In composition from 1.05 for $x = 0$ to 12.6 for $x = 0.15$. In fact, when In composition increases, the QW is pushed down near the conduction band edges in the contact layers, and the right contact depletion region slightly reduces, meanwhile the left one becomes somewhat larger (fig. 4(a)). Additionally, the applied bias is red-shifted and the value of the valley current is rather reduced. We point out that the current peak value varies in a less extend when increasing x due to its resonant nature which explains the low obtained PVR values. Results are summarized in table 3. Dashes in the table indicate that no peak is observed.

Comparing the present results (series B, $L_B = 0.6\,nm, L_Q = 0.8\,nm$) and those obtained in section 3-1 (series A, $L_B = 1\,nm, L_Q = 2\,nm$), it is clear that they present many differences. First, the transmission probability curves are different because the transmission coefficient depends essentially on the quasibound states in the QW. Indeed, reducing the width of the quantum well, the number of the quasibound states decreases and their

corresponding energy position is blueshifted far from the Fermi level in the contacts. As a consequence, the transmission peaks appear more deep and sharp when we use the dimension $L_B = 1\ nm$ and $L_Q = 2\ nm$ than $L_B = 0.6\ nm$, and $L_Q = 0.8\ nm$. Second, the position of resonant current peaks versus the applied bias are not the same since the voltage required to align the Fermi level in the contact layers with the QW quasibound states intensely depends on the conduction band profiles. The last difference is of a special interest since it affects the PVR values. In fact, in the first studied structures (series A, $L_B = 1\ nm, L_Q = 2\ nm$), the conduction band profile is very affected by indium composition and the device structure tends to become more symmetric, leading to a significant resonance transmission. Moreover, as it is shown in table 2, the difference between the peak and valley current is more pronounced which enhances the PVR. However, in the case of the present heterostructures of series (B) ($L_B = 0.6\ nm,\ L_Q = 0.8\ nm$), the conduction band profile is slightly affected by composition and the profile remains asymmetric which lowers the transmission through the resonant state. Consequently, as is it is displayed in table 3, the difference between the peak and valley current is not important and the PVR values are low in comparison with those given in table 2.

Table 3: Values of $J - V$ calculation of heterostructures series (B) at 300 K.

Series(B) (L_B, L_Q) = (1nm, 2nm)	**x (%)**	**Current density (A/cm²)**		**Tension (V)**		**PVR**
		Peak	Valley	Peak	Valley	
B_1	0	---	---	---	---	1
B_2	0.05	$1{,}47\times10^{6}$	$6{,}42\times10^{5}$	4,5	5,1	2,28
B_3	0.1	$1{,}72\times10^{6}$	$3{,}53\times10^{5}$	3,6	4,3	4,9
B_4	**0.15**	**$1{,}04\times10^{6}$**	**$8{,}3\times10^{4}$**	**3**	**3,7**	**12,6**

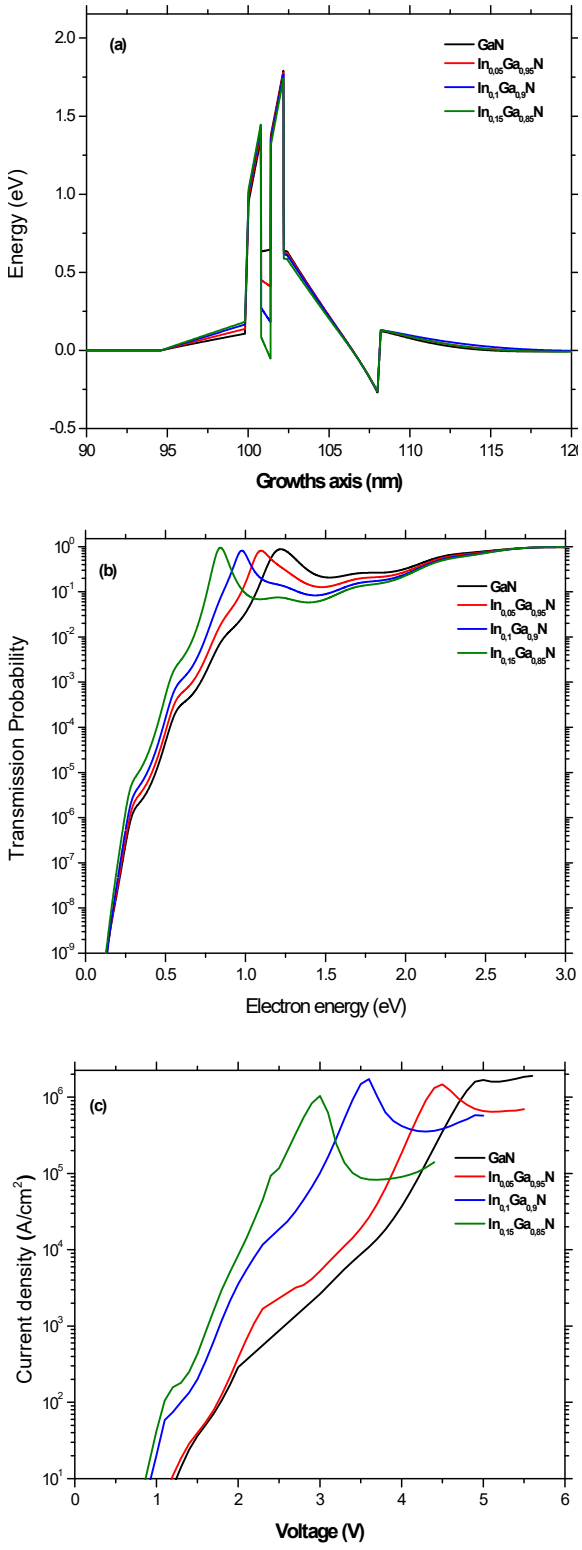

Figure 4: Results of: (a) Self consistent calculation of the equilibrium conduction band edge at zero bias, (b) transmission probability, and (c) current density for different In compositions in the n^+ (5.10^{18} cm^{-3})–GaN/5nm GaN/0.6 nm $Al_{0.5}G_{0.5}N$ /0.8 nm $In_xGa_{1-x}N$ /0.6 nm $Al_{0.5}G_{0.5}N$ / n^+ (5.10^{18} cm^{-3}) 6nm $In_{0.1}Ga_{0.9}N$ / n^+ (5.10^{18} cm^{-3}) GaN quantum structures.

3-3 Doping effects

Another important parameter that affects the electronic properties of resonant tunneling diodes is the carrier density (N_D) at both contact regions. We investigate heterostructures of identical geometry as those of series A and series B, however with N_D equal to $1 \times 10^{19}\ cm^{-3}$ in the asymptotic regions, with the aim to bring out the effect of the doping profiles on the current density ($J - V$).

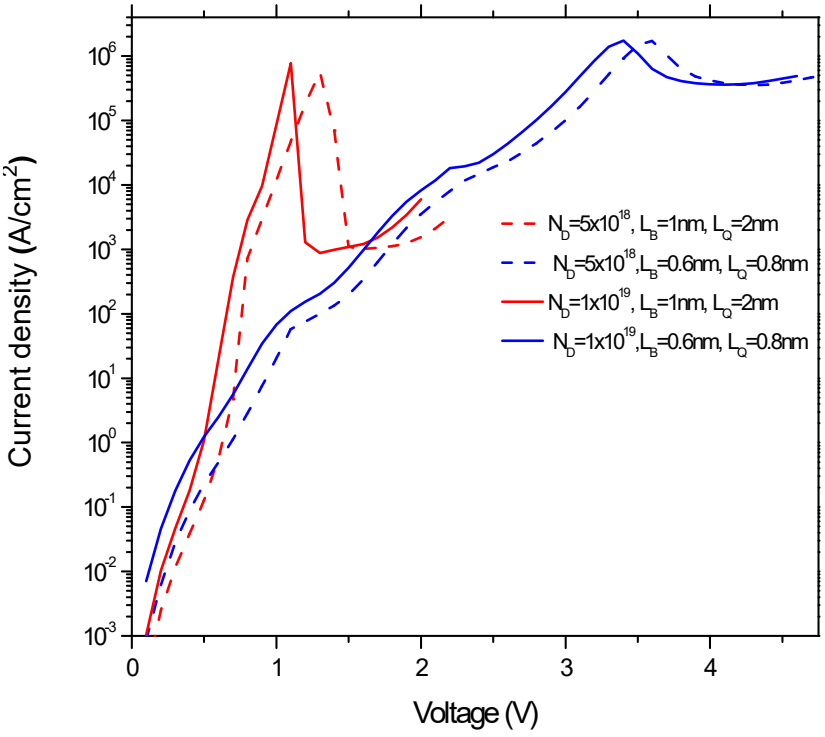

Figure 5: Theoretical $J-V$ curves calculated for different doping concentration and for indium composition $x = 0.1$.

A comparison with the results obtained with lower doping level is given in figure 5 for the In molar fraction of 10% (A_3 and B_3). In table 4 are displayed the Calculated PVR values for structures set (A) and set (B). At 300 K, the PVR is considerably enhanced to 882 for $x = 0.1$ for structures set (A) as compared to 564 from the previous results. However, The PVR is practically unchanged for structures set (B). As one can realize from figure 5, the importance of increasing the doping concentration is more prominent in structures with wide well and barriers where the peak current is significantly improved in comparison to the current valley which remains practically constant. Moreover, it can be seen that, at structure with highly doping concentration, the resonance is reached at lower bias.

Thus, we must conclude that, in view of peak-to-valley ratios, highly doped contacts and $In_{0.1}Ga_{0.9}N$ corrected spacer combined with large well thicknesses is of interest and should be considered.

Table 4: PVR values calculated at different doping concentration.

Series	x (%)	PVR	
		$5x10^{18}$ cm^{-3}	$1x10^{19}$ cm^{-3}
A_1	0	62	73,5
A_2	5	90	275
A_3	**10**	**564**	**882**
A_4	15	131.1	188.25
B_1	0	---	---
B_2	5	2.28	2.3
B_3	10	4.9	5
B_4	15	12.6	12.7

4 Conclusions

In summary we study a number of nitride based resonant tunneling diodes with different geometry. We have shown that a thin $In_{0.1}Ga_{0.9}N$ corrected spacer layer embedded between the second barrier and the top contact layers in the conventional and symmetric $GaN/Al_{0.5}Ga_{0.5}N$ RTD can bring advantages through polarization modulation and leads to better RTD performance.

Moreover, we propose using $In_xGa_{1-x}N$ material instead of GaN as the material of the central quantum well. We find that $J-V$ characteristics responds to modification of In composition, well and barrier thicknesses and also of doping concentration in the contact region. We show that an optimal design in terms of compositions, thicknesses and doping of the proposed resonant tunneling structure may allow a peak-to-valley ratio as high as 882 @1.1-1.3Volts. Ultimately the proposed $Al_{0.5}G_{0.5}N/In_xGa_{1-x}N/Al_{0.5}G_{0.5}N/In_{0.1}Ga_{0.9}N/GaN$ quantum structure provides a larger flexibility in the growth of GaN-based RTD heterostructures and can be further optimized in maximizing the room temperature peak-to valley ratio.

REFERENCES

[1] H. Zhao, R. A. Arif, Y. K. Ee, and N. Tansu, IEEE journal of quantum electronics, **45**, 66 (2008).

[2] F. Wu, W. Tian, W. Y. Yan, J. Zhang, S. C. Sun, J. N. Dai, Y. Y. Fang, Z. H. Wu and C. Q. Chen, J. Appl. Phys. **113**, 154505 (2013).

[3] E. Bellotti et al., J. Appl. Phys. **105**, 113103 (2009).

[4] F. Bernardini, and V. Fiorentini, Phys. Stat. Sol. (b), **216** (1999).

[5] F. Bernardini, and V. Fiorentini, **166**, 23 (2000).

[6] S. Sakr, E. Warde, M. Tchernycheva, and F. H. Julien, Appl. Phys. Lett. **99**, 142103 (2011).

[7] K. Berland, T. G. Andersson, and P. Hyldgaard, Phys. Rev. B **84**, 245313(2011).

[8] J.-G. S. Demers and R. Maciejko, J. Appl. Phys. **90**, 6120 (2001).

[9] R. Tsu and L. Esaki, Appl. Phys. Lett. **22**, 562 (1973).

[10] I. Vurgaftman and J. R. Meyer, J. Appl. Phys. **94**, 3675 (2003).

[11] I. Vurgaftman and J. R. Meyer, J. Appl. Phys. **89**, 5815 (2001).

[12] V. Bougrov et al, John Wiley & Sons, Inc, New York Chapter 1 (2001).

[13] B. Foutz, S. O'Leary, M. Shur, and L. Eastman, J. Appl. Phys. **85**, 7727 (1999).

[14] V.A. Fonoberov et al, J. Appl. Phys. **94**, 7178 (2003).

[15] Chin et al., J. Appl. Phys. **75**, 7365 (1994).

[**16**] O. Ombacher et al, J. Phys.: Condens. Matter. **14**, 3399 (2002).